Published in final edited form as:

Hippocampus. 2017 October ; 27(10): 1110–1122. doi:10.1002/hipo.22756.

Optogenetic stimulation of dentate gyrus engrams restores memory in Alzheimer's disease mice

Jennifer N. Perusini[a,b], **Stephanie A. Cajigas**[a], **Omid Cohensedgh**[a], **Sean C. Lim**[b,c], **Ina P. Pavlova**[b], **Zoe R. Donaldson**[a,b,d], and **Christine A. Denny**[a,b,*]

[a]Department of Psychiatry, Columbia University, New York, NY, U.S.A

[b]Division of Integrative Neuroscience, New York State Psychiatric Institute (NYSPI) / Research Foundation for Mental Hygiene, Inc. (RFMH), New York, NY, U.S.A

[c]Department of Neuroscience, MD-PhD Program, College of Physicians & Surgeons, Columbia University Medical Center, New York, NY, U.S.A

[d]Department of Molecular, Cellular, and Developmental Biology; Department of Psychology and Neuroscience, University of Colorado, Boulder, CO, U.S.A

Abstract

Alzheimer's disease (AD) is a prevalent neurodegenerative disorder characterized by amyloid-beta (Aβ) plaques and tau neurofibrillary tangles. APPswe/PS1dE9 (APP/PS1) mice have been developed as an AD model and are characterized by plaque formation at 4-6 months of age. Here, we sought to better understand AD-related cognitive decline by characterizing various types of memory. In order to better understand how memory declines with AD, APP/PS1 mice were bred with ArcCreER^{T2} mice. In this line, neural ensembles activated during memory encoding can be indelibly tagged and directly compared with neural ensembles activated during memory retrieval (i.e., memory traces/engrams). We first administered a battery of tests examining depressive- and anxiety-like behaviors, as well as spatial, social, and cognitive memory to APP/PS1 × ArcCreER^{T2} × channelrhodopsin (ChR2)-enhanced yellow fluorescent protein (EYFP) mice. Dentate gyrus (DG) neural ensembles were then optogenetically stimulated in these mice to improve memory impairment. AD mice had the most extensive differences in fear memory, as assessed by contextual fear conditioning (CFC), which was accompanied by impaired DG memory traces. Optogenetic stimulation of DG neural ensembles representing a CFC memory increased memory retrieval in the appropriate context in AD mice when compared with control (Ctrl) mice. Moreover, optogenetic stimulation facilitated reactivation of the neural ensembles that were previously activated during memory encoding. These data suggest that activating previously learned DG memory traces can rescue cognitive impairments and point to DG manipulation as a potential target to treat memory loss commonly seen in AD.

Corresponding Author: Christine Ann Denny, Ph.D., Address: Columbia University / RFMH, 1051 Riverside Drive, Unit 87, NYSPI Kolb Research Annex, Room 777, New York, NY 10032, Phone: (646) 774-7100, Fax: (646) 774-7102, cad2125@cumc.columbia.edu.

Finanacial Disclosures: The authors declare that they have no actual or potential conflicts of interest.

Keywords

Alzheimer's; hippocampus; Arc; engram; optogenetics

Introduction

AD is a prevalent neurodegenerative disorder impacting over 5 million people in the US. Memory deficits are evident in the earliest stages (e.g., decreased ability to remember names; misplaced objects). This progresses to major gaps in memory of recent and remote experiences and diminished awareness of surroundings. AD patients also have difficulty recognizing friends and family and often withdraw from social engagement (Reisberg et al., 1982; Chung and Cummings, 2000; Hargrave et al., 2002). In addition to the human suffering caused by the disease, AD has placed an enormous financial burden on the healthcare system and on patients' families.

AD pathology is characterized by Aβ peptide plaques and tau neurofibrillary tangles (Serrano-Pozo et al., 2012). The Aβ hypothesis of AD stipulates that Aβ aggregates form neurotoxic amyloid plaques, leading to neurodegeneration and dementia (Hardy and Allsop, 1991). The strongest evidence for this comes from molecular genetic studies of amyloid precursor proteins (APPs) and presenilins 1 and 2 (PS1, PS2) in early-onset familial AD, showing that all genetically-linked AD mutations increase the propensity for Aβ to aggregate *in vitro* (Selkoe, 2001). Mice with both the APPswe and PS1dE9 mutant transgenes have been previously developed (Jankowsky et al., 2001), with Aβ deposition appearing as early as 4 months of age (Jankowsky et al., 2004). These mice model multiple aspects of AD; they have poor coordination using a rotarod (Volianskis et al., 2010), contextual memory deficits (Gong et al., 2004; Kilgore et al., 2010) and impaired spatial learning in the Morris water maze (Gong et al., 2004; Lalonde et al., 2005). While this mouse line has been commercially available for some time, a complete behavioral analysis has not yet been performed to uncover the extent of behavioral and memory deficits with AD progression.

Growing evidence points to a link between the immediate early gene (IEG) *Arc/Arg3.1* and AD. Arc is predominantly expressed in cortical and hippocampal glutamatergic neurons and is required for LTP maintenance and memory consolidation (Lyford et al., 1995; Guzowski et al., 2000; Steward and Worley, 2001). Rodent studies report decreased IEG expression in cortical and hippocampal regions with AD (Rudinskiy et al., 2012; Palop et al., 2005). Wu et al. (2011) showed that Arc expression is required for the activity-dependent Aβ generation and for APP dysfunction. Furthermore, individuals with a novel Arc single nucleotide polymorphism reportedly have a reduced risk of AD (Landgren et al., 2012). Since Arc expression has been directly tied to AD, here, we proposed to utilize Arc expression as proxy of neuronal activity in order to localize AD-related memory deficits.

We previously generated a murine line that can be used to tag individual memories. The ArcCreER^{T2} mice can indelibly tag neural ensembles activated during learning with EYFP, and these populations can then be compared with those activated during memory retrieval, as labeled using Arc or c-Fos protein (Denny et al., 2014). This line is unique in that, unlike

most existing tools (e.g., Reijmers et al., 2007), it allows for the *permanent* labeling of activated neural ensembles, thereby permitting long-term or age-related studies. Using the ArcCreER^{T2} mice, we previously demonstrated that neuronal ensembles in the DG and CA3 hippocampal subregions are necessary for memory expression, and these memory traces are impacted by context, time, and adult hippocampal neurogenesis (Denny et al., 2014). Moreover, we have recently improved our protocols to tag neuronal ensembles by using superior pharmacological targeting windows, allowing for more specific studies (Cazzulino et al., 2016).

Here, we first administered an array of behavioral tests to the APP/PS1 × ArcCreER^{T2} × ChR2-EYFP mice in order to better understand how AD impacts behavior and memory as the disease develops. We hypothesized that if any deficits exist, they would be evident in the oldest age group, as plaque number increases. We found substantial deficits in social, spatial, and cognitive memories with onset of plaque development, with the most extensive quantifiable changes being in CFC. CFC deficits were accompanied by normal levels of EYFP and Arc labeling in the DG but by decreased EYFP^{+}/Arc^{+} co-labeling, suggesting a decreased recruitment of the original CFC memory trace. These data suggest that AD cognitive impairments result from weakened memory traces in that the memory is originally stored correctly in the brain, but cannot be properly accessed. The CFC memory deficits were rescued via optogenetic activation of the previously-encoded DG-dependent CFC memory trace. These findings support the hypothesis that targeting or stimulating the DG may be a successful method to treat memory loss, particularly cognitive or contextual memory loss, in AD.

Materials and Methods

Mice

ArcCreER^{T2}(+) mice (18) (predominantly 129S6/SvEv) were bred with ROSA26-CAG-stop^{flox}-ChR2(H134R)-EYFP (Ai32) (Madisen et al., 2012) (predominantly 129S6/SvEv but mixed with C57BL/6). Triple transgenic lines were then generated in which male ArcCreER^{T2}(+) × ChR2-EYFP homozygous (f/f) mice were bred with a mouse model of AD, female B6.Cg-Tg(APPswe; PSEN1dE9) 85Dbo/Mmjax (APP/PS1) mice (034832-JAX, MMRRC) (Jankowsky et al., 2004). This APP/PS1 line (on a C57BL/6 background) had a relatively high incidence of seizures (Minkeviciene et al., 2009). By crossing these mice with ArcCreER^{T2} mice, which are primarily bred on a 129S6/SvEv background, we were able to significantly reduce seizure frequency (data not shown). Male mice were used in all experiments. The Ctrl mice were: APP/PS1(-) × ArcCreER^{T2}(+) or (-) × ChR2-EYFP(+/f). The AD mice were: APP/PS1(+) × ArcCreER^{T2}(+) or (-) × ChR2-EYFP(+/f).

Genotyping

The Cre and ChR2 genotyping was performed as previously described (Denny et al., 2014). The APP and PSEN genotyping was performed as described on the Jackson Laboratory website. All genotyping was performed separately.

Standard Housing and Dark Housing

Mice were housed 4-5 per cage in a 12-h (06:00–18:00) light-dark colony room maintained at 22°C. Food and water were provided *ad libitum*. Behavioral testing was performed during the light phase. Each cohort was tested at the specific age to which it was assigned and mice were not tested at multiple ages.

Dark housing procedures occurred as previously described (Denny et al., 2014). Briefly, mice were dark housed the night before and then for 3 days following the 4-OHT injection. This allows for specific labeling of Arc^+ cells, as it limits other stimuli from turning on Arc. The procedures described herein were conducted in accordance with the National Institutes of Health regulations and approved by the Institutional Animal Care and Use Committees of Columbia University and the New York State Psychiatric Institute.

Behavioral Tests

Behavioral assays were performed on 2-, 4-, and 6-month-old mice. These assays were administered over 10 days. Please see Table S1 for the behavioral assays, as well as Supplemental Methods for additional behavioral tests and modified versions of the tests.

Contextual Fear Conditioning (CFC)

The 1- and 3-shock CFC protocols were administered as previously described (Drew et al., 2010; Denny et al., 2012). For the 1-shock CFC protocol, mice were placed into the conditioning chamber, received 1 shock at 180 s (2 s, 0.75 mA), and were removed 15 s following the shock. For the 3-shock CFC procedure, mice were placed in the conditioning chamber, received 3 shocks 180, 240, and 300 s later (2 s, 0.75 mA), and were removed 15 s following the last shock.

Drugs

Recombination was induced with 4-hydroxytamoxifen (4-OHT) (Sigma, St. Louis, MO). 4-OHT was dissolved by sonication in 10% EtOH/90% corn oil at a concentration of 10 mg/ml; each mouse was injected intraperitoneally (i.p.) with 200 μl (2 mg) (Cazzulino et al., 2016).

Mice were given an i.p. injection of Methoxy-X04 (5 mg/kg; Tocris Bioscience, Minneapolis, MN) 24 h prior to sacrifice to label plaques (Meyer- Luehmann et al., 2008). This procedure was adapted from Rudinskiy et al. (2012).

Immunohistochemistry

Brains were processed as previously described (Denny et al., 2014; Cazzulino et al., 2016).

Cell Quantification

An investigator blind to treatment used a Zeiss Axioplan-2 upright microscope to count immunoreactive cells bilaterally in the DG throughout the entire rostrocaudal axis as previously described (Denny et al., 2014; Cazzulino et al., 2016).

Confocal Microscopy

Fluorescent confocal micrographs were captured with a Leica TCS SP8 MP microscope as previously described (Cazzulino et al., 2016). To obtain the percent of reactivated cells, the total numbers of Arc^+ and $EYFP^+$ cells were counted in each confocal image. The number of Arc^+ cells that were co-labeled with $EYFP^+$ was then counted. The ratio is expressed as $((EYFP^+/Arc^+) / Arc^+) \times 100\%$.

Stereotaxic Surgery

Male mice were surgically implanted as previously described (Denny et al., 2014). Briefly, mice were implanted bilaterally with chronically dwelling optical fibers targeted to the DG (+/−1.0 mm ML, −1.5 mm AP, −1.7 mm DV).

Optogenetic Stimulation

Mice were first habituated to the fiber optic patch cables, attached bilaterally via zirconia sleeves, four times in their home cages. For stimulation during testing, the patch cables were interfaced to an FC/PC rotary joint (Doric lenses, Quebec, CAN), which was attached on the other end to a 473-nm laser diode. During the light ON epoch, blue light was provided for 3 min at a light power of 2-3 mW, 10 Hz, at 20 ms pulses at the tip of the implanted fiber optic.

Statistical Analysis

All data were analyzed using StatView (v. 5.0) software (SAS Institute). Data were analyzed using ANOVA, with repeated measures where appropriate. For each behavioral test, *a priori* planned comparisons (i.e., planned orthogonal contrasts) were performed for each age group in order to highlight genotype comparisons at each age and to test the hypothesis that behavioral deficits worsen with plaque development. For the regression analyses, the average CFC freezing versus either $EYFP^+$, Arc^+, or average co-labeled cells were plotted for each individual mouse. R^2 and p values are noted. Alpha was set to 0.05 for all analyses. Data are expressed as means ± SEM. All statistical tests are included in Table S2.

Results

AD disease progression as evidenced by amyloid deposits increases from 2 to 6 months of age

The APP/PS1 model (Jankowsky et al., 2014) was utilized and bred with the $ArcCreER^{T2}$ (Denny et al., 2014) × ChR2-EYFP (Madisen et al., 2012) mouse line (Fig. 1A). The mice were aged to 2, 4, or 6 months for behavioral assessment (Fig. 1B). Sample hippocampal micrographs with EYFP and Arc staining are shown for AD mice at all three ages (Fig. 1C). Amyloid expression was qualitatively characterized and used to verify AD progression by injecting Methoxy-X04, a derivative of Congo Red and Chrysamine-G (Klunk et al., 2002), 24 h before sacrifice. Methoxy-X04 deposits were observed in both 4- and 6-month old AD mice, but not in 2-year old mice (Fig. 1C). The number and size of Methoxy-X04 deposits also increased with age, which is consistent with previous studies (Volianskis et al., 2010; Garcia-Alloza et al., 2006).

Depressive- and anxiety-like behavior is not altered by AD

The forced swim test (FST) was utilized to determine if AD impacts depressive-like behavior. On day 1, all mice had comparable immobility times (data not shown). On day 2, while there was a significant effect of Age, there was no effect of Genotype or of the Genotype × Age interaction (Fig. 2A-2C). Average immobility time for minutes 3-6 on day 2 was comparable for Ctrl and AD mice (Fig. 2D-2F).

Next, the open field (OF), elevated plus maze (EPM), and novelty suppressed feeding (NSF) tests were administered to assess the impact of AD on anxiety-related behaviors. During the OF, basic movements were not affected by Age or Genotype (Fig. 2G-2I). All mice traveled similar distances in the center (Fig. 2J-2L). In the EPM, all mice, with the exception of 6-month-old AD mice, spent significantly more time in the closed arms than in the open arms (Fig. 2M-2O). In the NSF paradigm, all groups showed similar latencies to approach the pellet before the maximum allotted time of 8 min (Fig. 2P-2R). There was a significant effect of Age, but not of Genotype, on body weight (Fig. 2S-2U). There was no effect of Age or Genotype on weight loss during the fast-preceding the NSF paradigm (Fig. 2V-2X). Moreover, with the exception of 4-month-old AD mice, all groups showed similar levels of consumption in the home cage (Fig. 2Y-2AA). These data suggest that AD does not significantly impact depressive- or anxiety-like behaviors at 2- to 6-months of age in the APP/PS1 mice.

Novelty detection is impaired by aging, but not AD

Novelty detection was tested by first administering a 2-trial novel object recognition (NOR) paradigm (Fig. 3A-3C) as we previously described (28). Ctrl and AD mice failed to detect the novel object (Fig. 3C), suggesting that in this murine line, more time is needed to sufficiently encode the initial two objects.

Next, a 5-trial NOR paradigm was administered to determine if increased exposures would allow mice to sufficiently encode the two objects (24) (Fig. 3D-3M). In this paradigm, mice were habituated to two objects for four exposures, followed by a single exposure with one familiar (constant) object and one novel object. All mice had similar levels of activity across exposures (Fig. 3E-3G). There was a significant effect of Age, but not of Genotype on object investigation during habituation (Fig. 3H-3J). During the replacement trial, both Ctrl and AD mice detected the novel object, as evidenced by increased novel object exploration when compared with that of the constant object (Fig. 3K-3M). These data indicate that novelty detection is not severely impacted by AD.

Spatial working memory and social recognition is impaired by AD

To test spatial memory, an unbaited Y-maze was utilized (Fig. 4A). At 2 months of age, both the Ctrl and AD mice explored the novel arm significantly more than the constant arm during the test trial (Fig. 4B). However, at 4 months of age, AD mice showed similar levels of exploration of both arms, while the Ctrl mice explored the novel arm significantly more than the constant arm (Fig. 4C). At 6 months of age, Ctrl and AD mice explored both arms similarly (Fig. 4D).

To ensure that mice were using contextual cues outside of the Y-maze, in a separate experiment, the Y-maze was rotated 180° between training and test trials (Fig. S1A). Ctrl mice showed equal exploration of both arms (Fig. S1B), suggesting that outside contextual cues do influence the arm distinction. Moreover, these data suggest that this version of the task is too complex and more training trials would be necessary for enhanced performance.

Next, to test social investigation and to ensure that Ctrl and AD mice able of detecting social stimuli, a 1-trial social investigation test was administered using juvenile male mice (Fig. S1C). The time exploring an empty cup or a cup containing a novel male mouse was measured. Ctrl and AD mice were capable of detecting and investigating a novel male mouse, as evidenced by increased investigation of the mouse (Fig. S1D).

We next tested social memory of ovariectomized female conspecifics with a social recognition (SR) paradigm for Ctrl and AD mice (Fig.4E). During trial 1, there was an effect of Age, but not of Genotype, on the amount of exploration for the novel mouse when compared with the empty cup (Fig. 4F-4H). During the second trial, at 2 months, both Ctrl and AD mice explored the novel mouse more than the familiar mouse (Fig. 4I). However, at 4 months, Ctrl but not AD mice explored the novel mouse more than the familiar mouse (Fig. 4J). At 6 months of age, both Ctrl and AD mice investigated the novel and familiar mouse equally (Fig. 4K). These data indicate that all mice show age related deficits in SR, but these are exacerbated and occur earlier in AD mice.

Contextual fear memory is impaired by AD and this correlated with impaired DG memory traces

Lastly, in order to test long-term contextual fear memory, either 1-shock or 3-shock CFC procedures were administered to Ctrl and AD mice (Fig. 5A). To create the indelible label of memory encoding, 4-OHT was injected 5 h prior to CFC (Fig. 5B). For the 1-shock CFC procedure, at 2 months of age, both Ctrl and AD mice had comparable, albeit low, levels of freezing during the context test which was administered 5 days after the 1-shock procedure. However, at 4 and 6 months, while freezing increased in general over that of 2-month-old mice, AD mice exhibited lower levels of freezing when compared with Ctrl mice (Fig. 5C). While this weak procedure produces variable freezing across age, memory retrieval using a 1-shock CFC protocol is impaired in AD mice at 4 and 6 months of age.

After the context test, the mice were sacrificed, and immunohistochemistry was performed to quantify EYFP (memory encoding), Arc (memory expression), and $EYFP^+/Arc^+$ co-labeling (memory traces) in the DG (Fig. 5D-5F). For 1-shock CFC, Age but not Genotype impacted the number of $EYFP^+$ cells; 2-month-old mice had less $EYFP^+$ DG cells when compared with 4- and 6-month-old groups (Fig. 5D). Neither Genotype nor Age impacted the number of Arc^+ cells (Fig. 5E). However, at 6 months of age, but not 2 or 4 months of age, AD mice had significantly less co-labeled DG cells than did Ctrl mice (Fig. 5F), suggesting that the originally-encoded memory trace was not being recalled properly and that the behavioral deficit was paralleled by impaired DG memory traces. Moreover, because 2-month old mice displayed similar EYFP and Arc DG levels to 4-month old mice and 6-month-old Ctrl mice, this suggests that these cells do not represent behavioral output but rather contextual memory.

For 3-shock CFC, there was an overall effect of Genotype on freezing behavior (Fig. 5G). At 2 and 4 months, Ctrl and AD mice showed comparable levels of freezing during the context test, which was administered 5 days after the initial 3-shock procedure. However, at 6 months, AD mice showed a robust decrease in freezing in the aversive context when compared with Ctrl mice (Fig. 5G). While not statistically significant, 6-month-old Ctrl mice froze slightly more than did the two younger age groups, contributing to the striking difference observed between genotype at this age. These data indicate that CFC memory retrieval using a stronger shock protocol is simultaneously most impaired in AD mice and strongest in Ctrl mice at 6 months of age.

Following the same procedure as for 1-shock CFC, mice were sacrificed after the context test, and immunohistochemistry was performed to quantify EYFP, Arc, and co-labeling in the DG (Fig.s 5H-5J). For 3-shock CFC, both Ctrl and AD mice had comparable expression of DG $EYFP^+$ and Arc^+ cells across all ages (Fig.s 5H-5I). However, at 6 months, AD mice had significantly less co-labeling in the DG when compared with Ctrl mice (Fig. 5J). These data suggest that CFC becomes impaired with age but that these deficits are more profound in AD mice. This is paralleled by altered DG memory traces at more advanced stages of plaque development.

To address the varied freezing across age and to determine which factors contributed to fear expression, simple regression analyses with all 1-shock and 3-shock CFC data were performed. For 6-month-old mice, the number of $EYFP^+$ and co-labeled cells in the DG, but not Arc^+ cells, positively correlated with freezing percentage (Fig. S2A-S2C; Table S2). This suggests that, in the oldest group, both the cells representing the originally-encoded memory and those representing the memory trace best predict freezing behavior.

Optogenetic stimulation of a CFC DG memory trace improves memory retrieval in 6-month-old mice

Given the robust behavioral and IEG differences observed between 6-month-old AD and Ctrl mice, we hypothesized that impaired 3-shock CFC is due to weakened contextual memory retrieval in the DG with AD and that optogenetic stimulation of the neural ensemble representing this encoded memory would improve memory retrieval. Six-month-old APP/PS1 × $ArcCreER^{T2}$ × ChR2-EYFP mice were implanted with fiber optics directly above the DG (Fig. 6A). Mice were injected with 4-OHT and, 5 h later, exposed to context A and given 3 shocks. (Fig. 6B). Mice were then exposed to context A without shocks 5 days after the initial 3-shock CFC training, first with optogenetic stimulation for 3 min (2-3 mW, 10 Hz stimulation at 20 ms pulses) and then with no optogenetic stimulation for 3 min. Optogenetically stimulating the DG in AD × $ArcCreER^{T2}$(-) (Cre- AD) mice did not impact freezing behavior, as AD mice froze significantly less than Ctrl mice (Fig. 6C). However, optogenetically stimulating the DG in AD × $ArcCreER^{T2}$(+) (Cre+ AD) mice increased freezing behavior throughout the session; AD and Ctrl mice froze at comparable levels (Fig. 6D-6E).

The following day, during a context test without light stimulation, Cre- AD mice froze significantly less than Cre- Ctrl mice (Fig. 6F). Moreover, Cre+ AD mice also froze significantly less than Cre+ Ctrl mice (Fig. 6G-6H). These data suggest that the

improvements seen during the previous optogenetic stimulation are not long-lasting and that increased optogenetic stimulation is needed if long-lasting cognitive improvements are possible.

In order to determine if the timing of laser presentation impacts behavior and to more definitively attribute increased freezing to laser stimulation, mice received laser OFF and then laser ON periods in context A (Fig. 6B). Cre- AD mice froze significantly less than Cre- Ctrl mice during the laser OFF and laser ON periods (Fig. 6I). Cre+ AD mice froze significantly less than Cre+ Ctrl mice during the laser OFF period (Fig. 6J). However, during the laser ON period, Cre+ AD mice froze comparably to Cre+ Ctrl mice, again suggesting that optogenetic stimulation is capable of rescuing the memory deficit in AD mice at any portion of the context test (Fig. 6J-6K). These data suggest that optogenetic stimulation of an aversive contextual memory trace rescues the 3-shock CFC memory impairment in AD mice, as evidenced by increased freezing in the shock context.

Lastly, mice were sacrificed after 10 min of laser stimulation, and immunohistochemistry was performed for Cre+ mice as previously described (Fig. 5). Both Cre+ Ctrl and AD mice had similar levels of DG EYFP and Arc expression (Fig. 6L-6N). However, stimulation increased overall DG co-labeling in Cre+ AD mice, significantly higher than impaired AD mice without stimulation (Table S2). This increased DG co-labeling reflects the behavioral improvements for Cre+ AD mice during optogenetic stimulation of the appropriate CFC memory trace. Moreover, for all Cre+ mice, irrespective of Genotype, co-labeling was significantly increased in DG sections directly under the ferrule (i.e., DG sections directly simulated by the laser) compared to those past the ferrule (i.e., DG sections not directly stimulated by the laser) (Fig. 6O). Therefore, these data show that optogenetic stimulation of DG engrams improves memory retrieval in AD mice by increasing the reactivation of neural ensembles which were active during memory encoding.

Discussion

AD has become a devastating societal and health problem among the elderly. In this study, we aimed to first characterize the time course of changes in multiple behavioral domains in an AD mouse model. Some behaviors were unaffected by plaque development, namely anxiety-like behaviors and novelty detection. However, we found that social, spatial, and cognitive memories were severely impaired with plaque progression. These data are in accord with other studies using similar AD murine lines. For example, spatial memory deficits using the water maze (Lalonde et al., 2005; Cao et al., 2007), as well as SR deficits (Hsaio et al., 2014), have been found in APP/PS1 mice. Most importantly, here, we report that one of the most robust and measurable deficits were in cognitive fear memory as assessed by CFC. This is consistent with human literature on AD-related memory dysfunction, especially as AD progresses into later stages (e.g., Koedam et al., 2010).

After both 1- and 3-shock CFC, DG EYFP and Arc expression were comparable across all groups despite behavioral memory deficits occurring at 6 months of age. Since we utilized a murine line that allows for indelible labeling of memory traces, we were able to compare neuronal populations active during memory encoding and retrieval. $EYFP^{+}/Arc^{+}$ co-labeling

(i.e., reactivated memory traces / engrams) was significantly decreased in 6-month-old AD mice when compared with the age-matched Ctrl mice. This implies that in this oldest age group with AD, the cells activated during context re-exposure were not the same as those activated during memory encoding. That is, the mice may be recalling an incorrect memory, as the wrong cells—or possibly a new ensemble that may have different mnemonic properties than the original ensemble—are being activated. False recollection and diminished memory accuracy, especially of those with emotional valence, are common in AD patients, and studies report these impairments are due to hippocampal dysfunction (e.g., Gallo et al., 2010). Interestingly, we observed slight freezing increases in aged Ctrl mice, which was most apparent in 3-shock CFC. While unexpected, this finding is supported by human literature stating that the aging population is more sensitive to the effects of stress (e.g., Wilson et al., 2011). Nonetheless, percent co-labeling was typical for this group (~8%; Denny et al., 2014), significantly higher than that of the age-matched AD group, and regression analysis showed that in this oldest group, both the cells representing the originally-encoded memory and those representing the memory trace were indeed predictors of fear expression.

We hypothesized that AD mice had deficits in CFC because the original encoding population was not reactivated properly during re-exposure, thereby incorrectly accessing the memory trace. By tagging the neural ensembles representing memory encoding, we tested if optogenetic stimulation of this population would be sufficient to improve memory retrieval. Indeed, optogenetic stimulation of this neural population increased fear memory retrieval as well as DG co-labeling (i.e., memory retrieval) to that of Ctrl levels. Increased co-labeling for Cre+ mice suggests that laser stimulation directly strengthens the memory trace, which is then reflected in improved behavior for AD mice. Moreover, these results indicate that the CFC memory still exists and has not degraded, but is difficult to access for memory retrieval or behavioral expression when AD is present. Because we were able to improve fear memory deficits in these studies, in the future it may be possible optogenetically stimulate neural ensembles representing SR or spatial memories to also improve these impairments in these triple transgenic mice.

Two recent studies are particularly relevant to interpreting our data. Firstly, a recent study similarly used optogenetics to reactivate fear memory traces in AD mice (Roy et al., 2016). In this study, the authors were able to also temporarily increase freezing during light stimulation; however, the stimulation was never performed in the CFC training context but in a completely novel context. It is unclear from the procedure whether they were activating the complete CFC engram or cells representing behavioral output (i.e., freezing). Here, we optogenetically stimulated cells labeled during CFC training in the same aversive context. With a procedure utilizing the same aversive context for both CFC training and memory recall, we provide a cleaner and more accurate comparison of cells active during encoding versus retrieval, which allows for a more meaningful interpretation of co-labeled cells. Moreover, we have shown that we can improve fear memory to unimpaired Ctrl levels within the relevant context and not an alternate one; testing in an alternate context could be inappropriate in practice or clinical instances. Secondly, a recent study also showed that optogenetically driving fast-spiking Parvalbumin^{+} hippocampal interneurons at gamma, but not other frequencies reduced the levels of Aβ (Iaccarino et al., 2016). These data suggest

that non-invasively targeting brain rhythms may improve memory retrieval by decreasing the AD-associated pathology. Altogether, both studies suggest that optogenetic modulation during AD progression results in improved memory and also highlights the hippocampus as a node of influence for improving long-term memory retrieval.

In summary, these data represent an in-depth behavioral and IEG profiling of the APP/PS1 murine model commonly used to study AD. We have identified distinct memory deficits that occur with AD progression. We believe that each of these behaviors (cognitive, spatial, and social) is mediated by distinct memory traces that will require distinct targeting procedures to potentially improve deficits. In the case of 1-shock and 3-shock CFC, we have localized memory trace impairments in the DG and optogenetically targeted the cells used to originally encode the CFC memory. This context-specific memory trace activation rescued memory retrieval, as indicated by the enhanced degree of IEG expression overlap. Overall, these findings propose that the DG is a prime target for treating AD-related cognitive decline.

Supplementary Material

Refer to Web version on PubMed Central for supplementary material.

Acknowledgments

J.N.P. was supported by a NIH DP5 OD017908 and NIH T32 MH015174. S.C.L. was supported by a NIH DP5 OD017908. I.P. was supported by a NYSTEM C-029157. C.A.D. was supported by a NIH DP5 OD017908-01, a NARSAD Young Investigator Grant from the Brain & Behavior Research Foundation (P&S Fund Investigator), a NYSTEM C-029157, a Research Initiatives for Science and Engineering (RISE) grant, and a Robert N. Butler Columbia Aging Center of Columbia University Faculty Research Fellowship.

References

Cao D, Lu H, Lewis TL, Ling L. Intake of sucrose-sweetened water induces insulin resistance and exacerbates memory deficits and amyloidosis in a transgenic mouse model of Alzheimer Disease. J Bio Chem. 2007; 282:36275–36282. [PubMed: 17942401]

Cazzulino AS, Martinez R, Tomm NK, Denny CA. Improved specificity of hippocampal memory trace labeling. Hippocampus. 2016; 26:752–62. [PubMed: 26662713]

Chung JA, Cummings JL. Neurobehavioral and neuropsychiatric symptoms in Alzheimer's disease: characteristics and treatment. Neuro Clin. 2000; 18:829–46.

Denny CA, Burghardt NS, Schachter DM, Hen R, Drew MR. 4- to 6-week old adult born hippocampal neurons influence novelty-evoked exploration and contextual fear conditioning. Hippocampus. 2012; 22:1188–1201. [PubMed: 21739523]

Denny CA, Kheirbek MA, Alba EL, Tanaka KF, Brachman RA, Laughman KB, Tomm NK, Turi GF, Losonczy A, Hen R. Hippocampal memory traces are differentially modulated by experience, time, and adult neurogenesis. Neuron. 2014; 83:189–201. [PubMed: 24991962]

Drew MR, Denny CA, Hen R. Arrest of adult hippocampal neurogenesis in mice impairs single- but not multiple-trial contextual fear conditioning. Behav Neurosci. 2010; 124:446–454. [PubMed: 20695644]

Gallo DA, Foster KT, Wong JT, Bennett DA. False recollection of emotional pictures in Alzheimer's disease. Neuropsychologia. 2010; 48:3614–3618. [PubMed: 20727904]

Garcia-Alloza M, Robbins EM, Zhang-Nunes SX, Purcell SM, Betensky RA, Raju S, Prada C, Greenberg SM, Bacskai BJ, Frosch MP. Characterization of amyloid deposition in the APPswe/PS1dE9 mouse model of Alzheimer's disease. Neurobiol Dis. 2006; 24:516–524. [PubMed: 17029828]

Gong B, Vitolo OV, Trinchese, Liu S, Shelanski M, Arancio O. Persistent improvement in synaptic and cognitive functions in an Alzheimer mouse model after rolipram treatment. J Clin Invest. 2004; 114:1624–1634. [PubMed: 15578094]

Guzowski JF, Lyford GL, Stevenson GD, Houston FP, McGaugh JL, Worley PF, Barnes CA. Inhibition of activity-dependent arc protein expression in the rat hippocampus impairs the maintenance of long-term potentiation and the consolidation of long-term memory. J Neurosci. 2000; 20:3993–4001. [PubMed: 10818134]

Hardy J, Allsop D. Amyloid deposition as the central event in the aetiology of Alzheimer's disease. Trends Pharmacol Sci. 1991; 12:383–388. [PubMed: 1763432]

Hargrave R, Maddock RJ, Stone V. Impaired recognition of facial expressions of emotion in Alzheimer's Disease. J Neuropsych Clin N. 2002; 14:64–71.

Hsaio YH, Hung HC, Chen SH, Gean PV. Social interaction rescues memory deficit in an animal model of Alzheimer's disease by increasing BDNF-dependent hippocampal neurogenesis. J Neurosci. 2014; 34:16207–16219. [PubMed: 25471562]

Iaccarino HF, Singer AC, Martorell AJ, Rudenko A, Gao F, Gillingham TZ, Mathys H, Seo J, Kritskiy O, Abdurrob F, Adaikkan C, Canter RG, Rueda R, Brown EN, Boyden ES, Tsai LH. Gamma frequency entrainment attenuates amyloid load and modifies microglia. Nature. 2016; 540:230–235. [PubMed: 27929004]

Jankowsky JL, Fadale DJ, Anderson J, Xu GM, Gonzales V, Jenkins NA, Copeland NG, Lee MK, Younkin LH, Wagner SL, Younkin SG, Borchelt DR. Mutant presenilins specifically elevate the levels of the 42 residue beta-amyloid peptide in vivo: evidence for augmentation of a 42-specific gamma secretase. Hum Mol Genet. 2004; 13:159–170. [PubMed: 14645205]

Jankowsky JL, Slunt HH, Ratovitski T, Jenkins NA, Copeland NG, Borchelt DR. Co-expression of multiple transgenes in mouse CNS: a comparison of strategies. Biomol Eng. 2001; 17:1157–1165.

Kilgore M, Miller CA, Fass DM, Hennig KM, Haggarty SJ, Sweatt JD, Rumbaugh G. Inhibitors of class 1 histone deacetylases reverse contextual memory deficits in a mouse model of Alzheimer's Disease. Neuropsychopharmacology. 2010; 35:870–880. [PubMed: 20010553]

Klunk WE, Bacskai BJ, Mathis CA, Kajdasz ST, McLellan ME, Frosch MP, Debnath ML, Holt DP, Wang Y, Hyman BT. Imaging Abeta plaques in living transgenic mice with multiphoton microscopy and methoxy-X04, a systemically administered Congo red derivative. J Neuropathol Exp Neurol. 2002; 61:797–805. [PubMed: 12230326]

Koedam EL, Lauffer V, van der Vlies AE, van der Flier WM, Scheltens P, Pijnenberg YA. Early-versus late-onset Alzheimer's disease: more than age alone. J Alzheimers Dis. 2010; 19:1401–1408. [PubMed: 20061618]

Lalonde R, Kim HD, Maxwell JA, Fukuchi K. Exploratory activity and spatial learning in 12-month-old APP_{695}SWE/co+PS1/ΔE9 mice with amyloid plaques. Neurosci Lett. 2005; 390:87–92. [PubMed: 16169151]

Landgren S, von Otter M, Palmér MS, Zetterström C, Nilsson S, Skoog I, Gustafson DR, Minthon L, Wallin A, Andreasen N, Bogdanovic N, Marcusson J, Blennow K, Zetterberg H, Kettunen P. A novel ARC gene polymorphism is associated with reduced risk of Alzheimer's disease. J Neural Transm. 2012; 199:833–842.

Lyford GL, Yamagata K, Kaufmann WE, Barnes CA, Sanders LK, Copeland NG, Gilbert DJ, Jenkins NA, Lanahan AA, Worley PF. Arc, a growth factor and activity-regulated gene, encodes a novel cytoskeleton-associated protein that is enriched in neuronal dendrites. Neuron. 1995; 14:433–445. [PubMed: 7857651]

Madisen L, Mao T, Zhuo JM, Berenyi A, Fujisawa S, Hsu YW, Garcia AJ 3rd, Gu X, Zanella S, Kidney J, Gu H, Mao Y, Hooks BM, Boyden ES, Buzsaki G, Ramirez JM, Jones AR, Svoboda K, Han X, Turner EE, Zeng H. A toolbox of Cre-dependent optogenetic transgenic mice for light-induced activation and silencing. Nat Neurosci. 2012; 15:793–802. [PubMed: 22446880]

Meyer-Luehmann M, Spires-Jones T, Prada C, Garcia-Alloza M, de Calignon A, Rozkalne M, Koenigsknecht-Talboo J, Holtzman DM, Bacskai BJ, Hyman BT. Rapid appearance and local toxicity of amyloid-beta plaques in a mouse model of Alzheimer's disease. Nature. 2008; 451:720–724. [PubMed: 18256671]

Minkeviciene R, Rheims S, Dobszay MB, Zilberter M, Hartikainen J, Fülöp L, Penke B, Zilberter Y, Harkany T, Pitkanen A, Tanila H. Amyloid β-induced neuronal hyperexcitability triggers progressive epilepsy. J Neurosci. 2009; 29:3453–3462. [PubMed: 19295151]

Oury F, Khrimian L, Denny CA, Gardin A, Chamouni A, Goeden N, Huang YY, Lee H, Srinivas P, Gao XB, Suyama S, Langer T, Mann JJ, Horvath TL, Bonnin A, Karsenty G. Maternal and offspring pools of osteocalcin influence brain development and functions. Cell. 2013; 26:228–241.

Palop JJ, Chin J, Bien-Ly N, Massaro C, Yeung BZ, Yu GQ, Mucke L. Vulnerability of dentate granule cells to disruption of arc expression in human amyloid precursor protein transgenic mice. J Neurosci. 2005; 25:9686–9693. [PubMed: 16237173]

Reijmers LG, Perkins BL, Matsuo N, Mayford M. Localization of a stable neural correlate of associative memory. Science. 2007; 317:1230–1233. [PubMed: 17761885]

Reisberg B, Ferris SH, de Leon MJ, Crook T. The Global Deterioration Scale for assessment of primary degenerative dementia. Am J Psychiatry. 1982; 139:1136–1139. [PubMed: 7114305]

Roy DS, Arons A, Mitchell TI, Pignatelli M, Ryan TJ, Tonegawa S. Memory retrieval by activating engram cells in mouse models of early Alzheimer's disease. Nature. 2016; 531:508–512. [PubMed: 26982728]

Rudinskiy N, Hawkes JM, Betensky RA, Eguchi M, Yamaguchi S, Spires-Jones TL, Hyman BT. Orchestrated experience-driven Arc responeses are disrupted in a mouse model of Alzheimer's disease. Nat Neurosci. 2012; 15:1422–1429. [PubMed: 22922786]

Selkoe DJ. Alzheimer's disease: genes, proteins, and therapy. Physiol Rev. 2001; 81:741–766. [PubMed: 11274343]

Serrano-Pozo, A., Frosch, MP., Masliah, E., Hyman, BT. Neuropathological Alterations in Alzheimer Disease. In: Selkoe, DJ.Mandelkow, EM., Holtzman, DM., editors. The Biology of Alzheimer Disease. Cold Spring Harbor, NY: Cold Spring Harbor Laboratory Press; 2012.

Steward O, Worley PF. Selective targeting of newly synthesized Arc mRNA to active synapses requires NMDA receptor activation. Neuron. 2001; 30:227–240. [PubMed: 11343657]

Volianskis A, Køstner R, Mølgaard M, Hass S, Jensen MS. Episodic memory deficits are not related to altered gluatmatergic synaptic transmission and plasticity in the CA1 hippocampus of the APPswe/PS1ΔE9-deleted transgenic mice model of β-amyloidosis. Neurobiol Aging. 2010; 31:1173–1187. [PubMed: 18790549]

Wilson RS, Begeny CT, Boyle PA, Schneider JA, Bennett DA. Vunerability to stress, anxiety, and development of dementia in old age. Am J Geriatr Psychiatry. 2011; 19:327–334. [PubMed: 21427641]

Wu J, Petralia RS, Kurushima H, Patel H, Jung MY, Volk L, Chowdhury S, Shepherd JD, Dehoff M, Li Y, Kuhl D, Huganir RL, Price DL, Scannevin R, Troncoso JC, Wong PC, Worley PF. Arc/Arg3.1 regulates an endosomal pathway essential for activity-dependent β -amyloid generation. Cell. 2011; 147:615–628. [PubMed: 22036569]

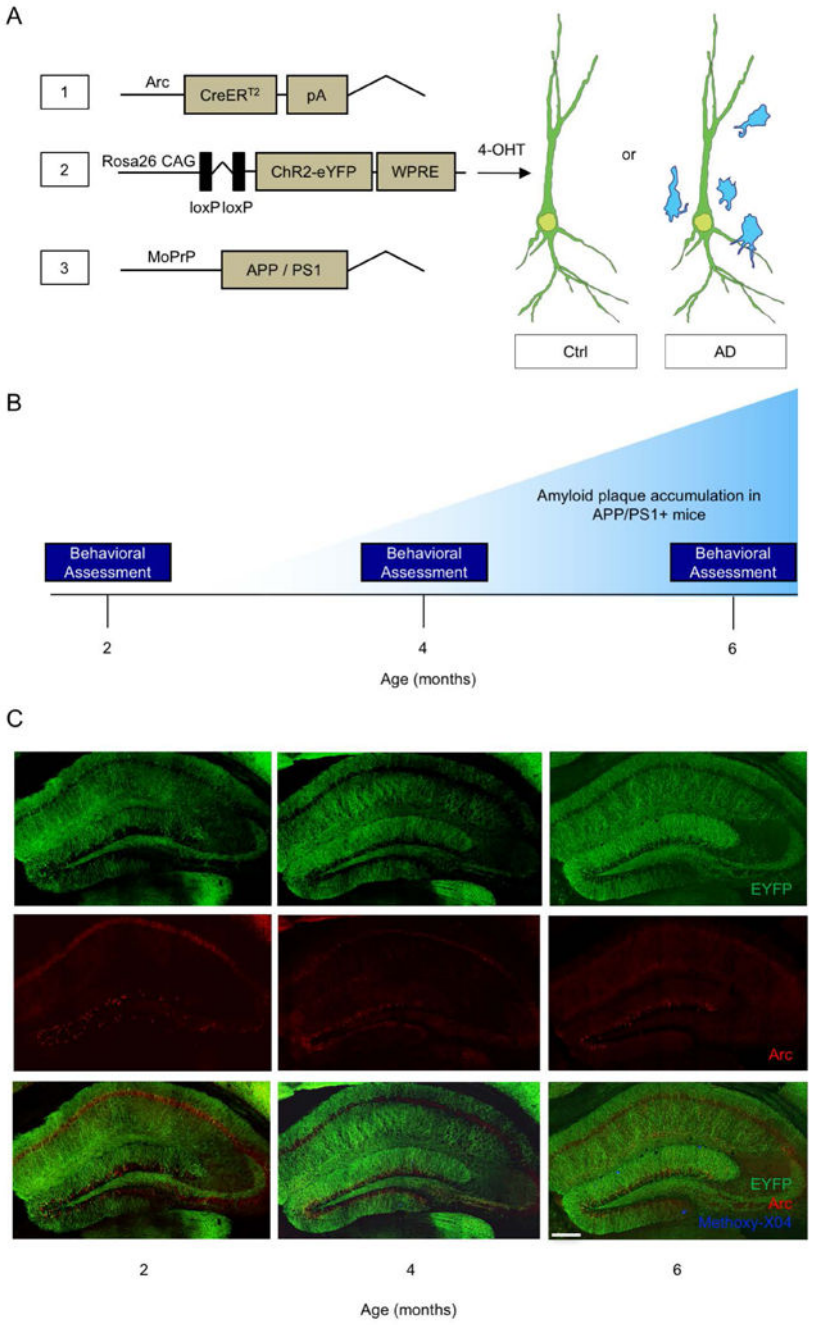

Figure 1. Experimental design for APP/PS1 (AD) × ArcCreER^{T2} × ChR2-EYFP mice

(A) Genetic design.

(B) Behavioral design.

(C) Representative images of EYFP, Arc, and Methoxy-X04 immunohistochemistry at 2, 4, and 6 months of age. Scale bar represents 100 μm.

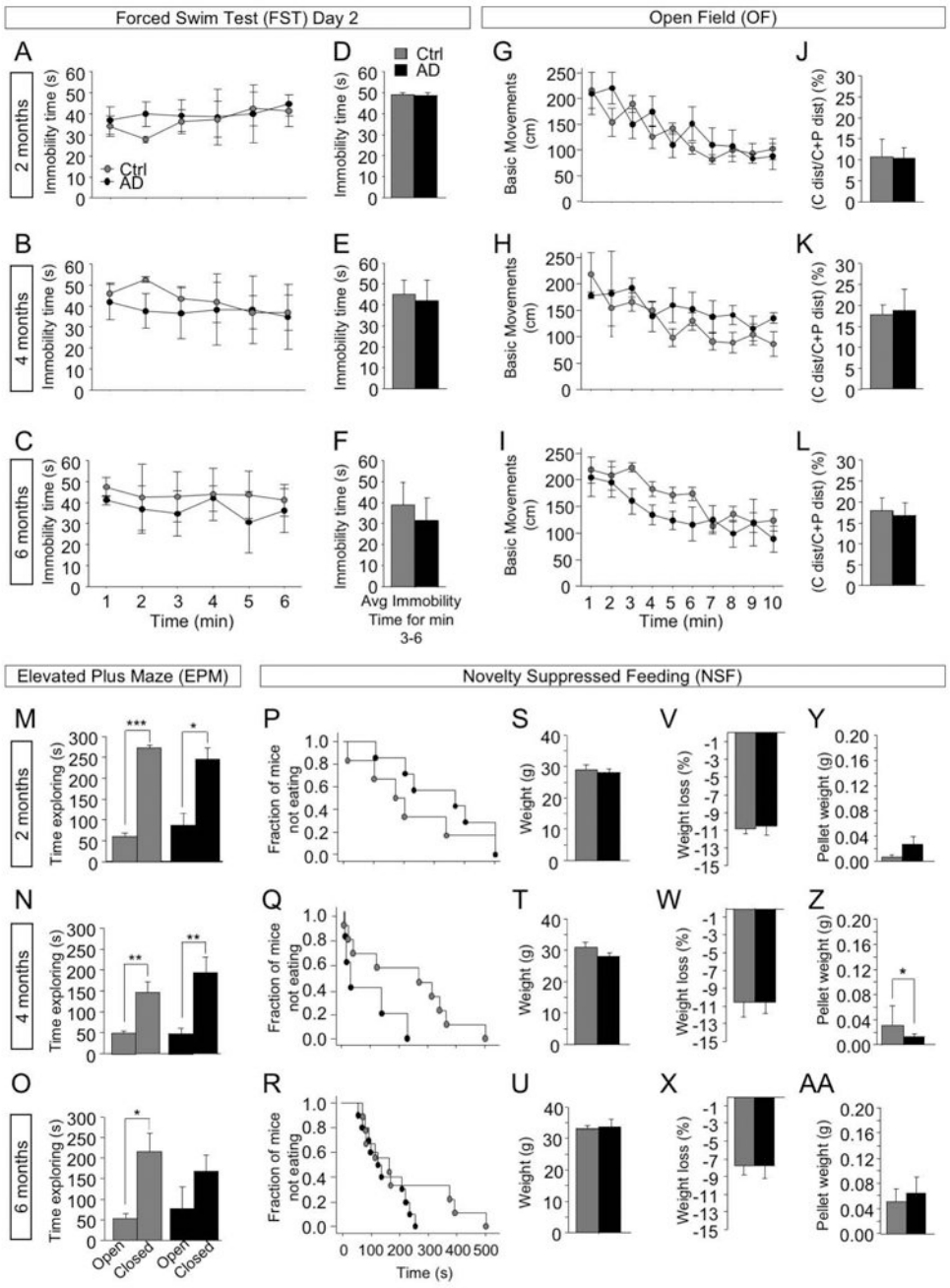

Figure 2. Depressive- and anxiety-like behavior is not altered in AD mice

(A-C) Ctrl and AD mice had similar levels of immobility time on day 2 of the FST.

(D-F) Ctrl and AD mice had similar levels of average immobility time for minutes 3-6 on day 2 of the FST.

(G-I) In the OF, Genotype did not impact basic movements at 2, 4, or 6 months of age.

(J-L) Neither Genotype nor Age impacted the distance traveled in the center over total distance traveled.

(M-O) Ctrl and AD mice spent more time in the closed arms of the EPM at all ages tested, except for the AD group at 6 months of age.
(P-R) For the NSF test, neither Genotype nor Age impacted the latency to eat a pellet.
(S-U) Ctrl and AD mice had comparable body weights at all ages measured.
(V-X) Ctrl and AD mice had comparable percentage of body weight loss.
(Y-AA) Ctrl and AD mice ate similar amounts of food in the home cage following the NSF. (n = 6-13 male mice per group). Error bars represent ± SEM. * $p < 0.05$, ** $p < 0.01$, *** $p < 0.001$. Forced Swim Test, FST; Open Field, OF; Elevated Plus Maze, EPM; Novelty Suppressed Feeding, NSF; Average, Avg; minutes, min; seconds, s; control, Ctrl; Alzheimer's disease, AD; gram, g; percent, %; centimeter, cm.

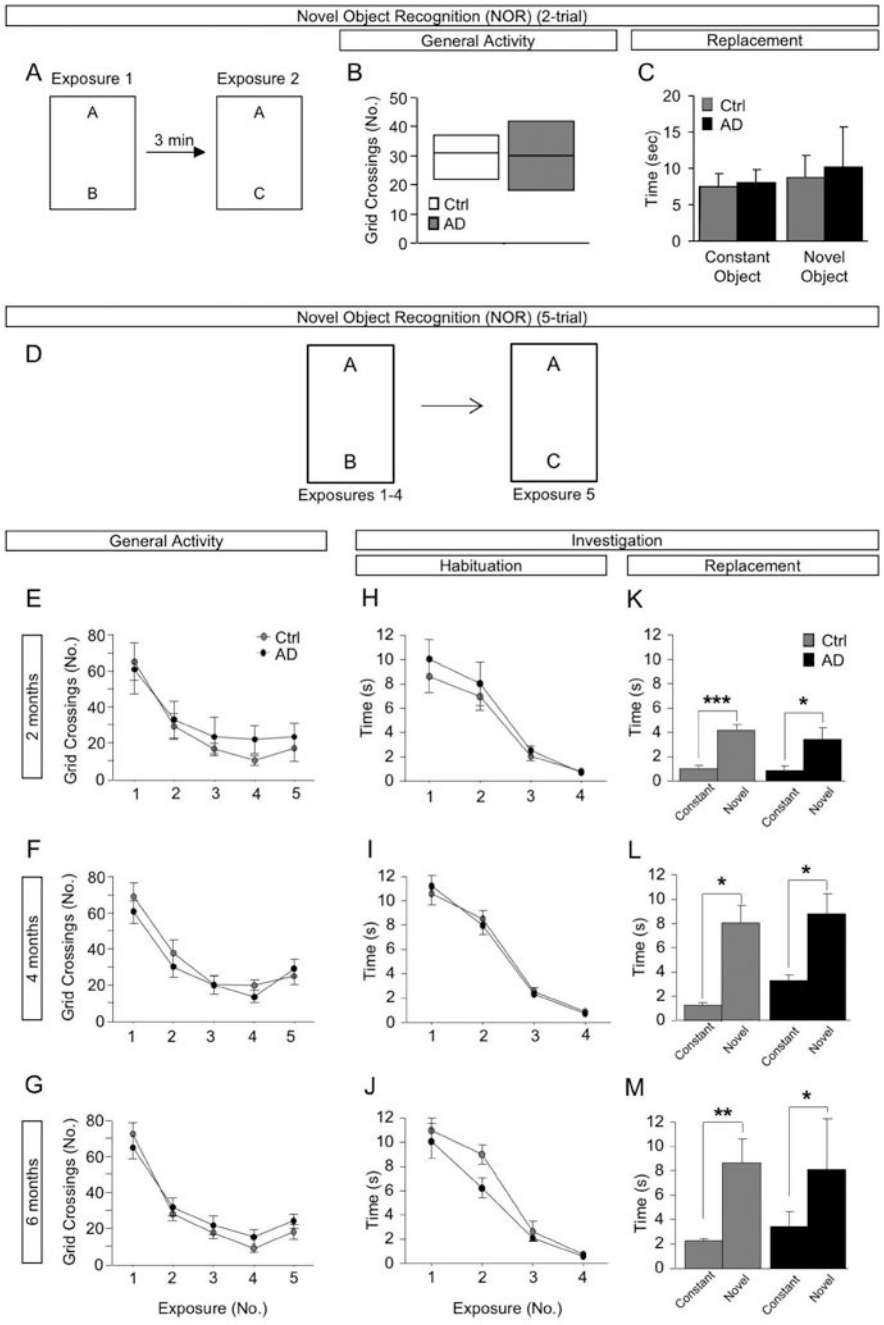

Figure 3. Aging and AD do not affect novelty detection in 2-trial NOR, but aging alters novelty detection in 5-trial NOR

(A) Experimental design.

(B) In exposure 2, Ctrl and AD mice had similar levels of exploration, as measured by grid crossings.

(C) Ctrl and AD mice had similar levels of investigation of the two objects, with both groups showing no preference for the novel object, suggesting that this paradigm is not sufficient for testing long-term NOR. (n = 3-4 male mice per group).

(D) Experimental design.

(E-G) Ctrl and AD mice had similar levels of exploration, as measured by grid crossings, at all ages measured.
(H-J) Ctrl and AD mice had similar levels of investigation of the two objects at all ages measured.
(K-M) Ctrl and AD mice investigated the novel object significantly more than the constant object at 2, 4, and 6 months of age. (n = 6-13 male mice per group). Error bars represent ± SEM. * $p < 0.05$, ** $p < 0.01$, *** $p < 0.001$. Minutes, min; Novel Object Recognition, NOR; control, Ctrl; Alzheimer's disease, AD; seconds, s; number, No.

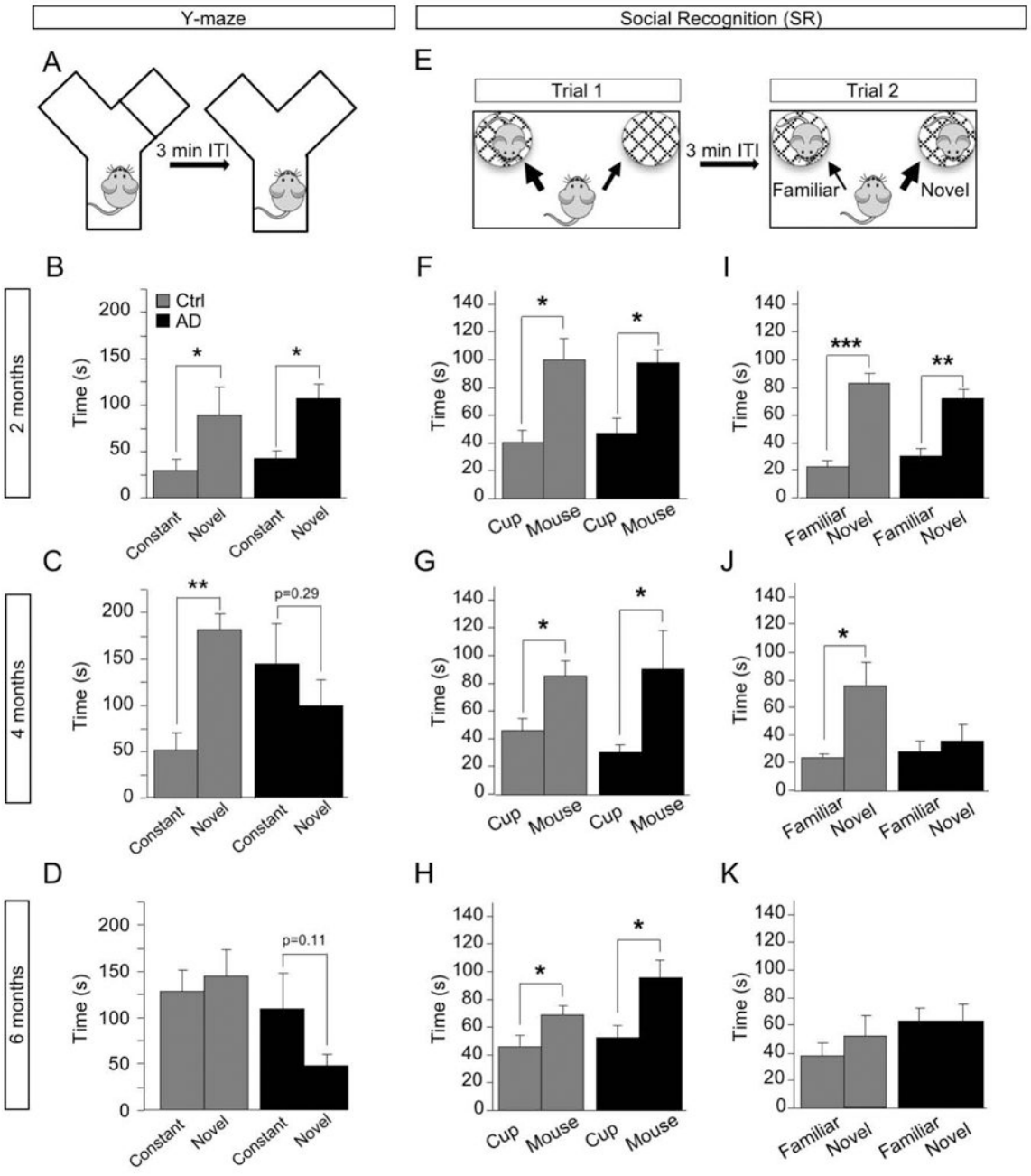

Figure 4. Spatial and social memories are altered with both aging and plaque onset

(A) Y-maze experimental design.

(B) Two-month-old Ctrl and AD mice explore the novel arm significantly more than the constant arm.

(C) At 4 months, Ctrl, but not AD mice explore the novel arm significantly more than the constant arm.

(D) At 6 months, both groups of mice explore the constant and novel arms comparably.

(E) SR experimental design.

(F-H) During trial 1, Ctrl and AD mice explore the novel mouse significantly more than the empty cup.
(I) At 2 months of age, Ctrl and AD mice explore the novel mouse significantly more than the familiar mouse during trial 2.
(J) At 4 months, Ctrl but not AD mice explore the novel mouse significantly more than the familiar mouse during trial 2.
(K) At 6 months, both groups of mice explore the novel and familiar mice comparably during trial 2. (n = 6-13 male mice per group). Error bars represent ± SEM. * $p < 0.05$, ** $p < 0.01$, *** $p < 0.001$. Control, Ctrl; Alzheimer's disease, AD; seconds, s; intertrial interval, ITI.

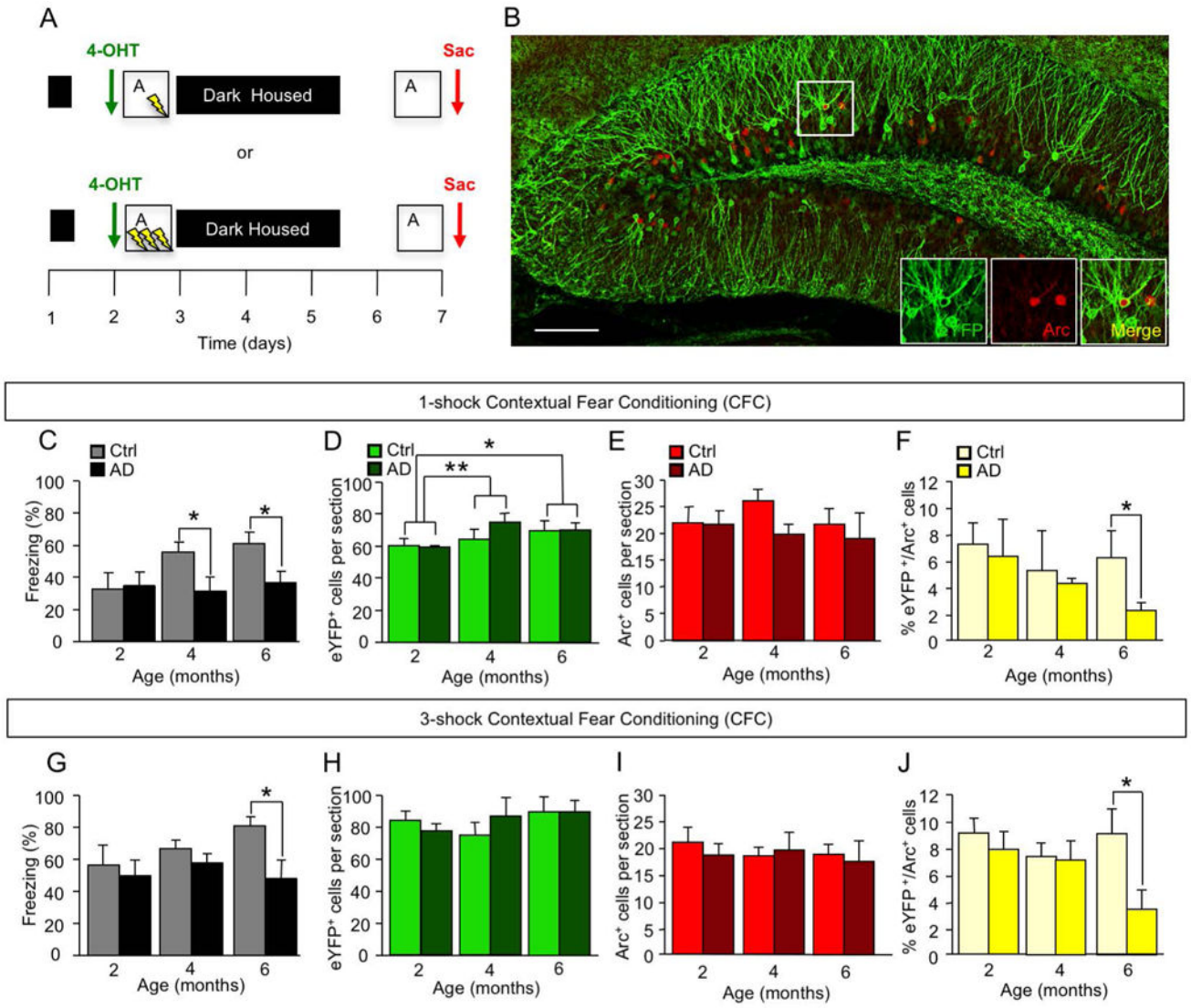

Figure 5. CFC and IEG expression is impaired in AD mice

(A) CFC experimental designs.

(B) Representative image of EYFP, Arc, and Methoxy-X04. Scale bar represents 100 microns.

(C) At 2 months of age, Ctrl and AD mice exhibit comparable freezing levels following1-shock CFC. At 4 and 6 months, AD mice exhibit significantly less freezing than Ctrl mice.

(D-E) There was no effect of Genotype on the number of $EYFP^+$ or the number of Arc^+ DG cells.

(F) At 6 months, AD mice have significantly less DG $EYFP^+/Arc^+$ co-labeling than do Ctrl mice.

(G) At 6 months, AD mice exhibit significantly less freezing than Ctrl mice following 3-shock CFC.

(H-I) There was no effect of Genotype on the number of $EYFP^+$ or the number of Arc^+ DG cells.

(J) At 6 months, AD mice have a significantly less co-labeling than Ctrl mice. (n = 6-13 male mice per group). Error bars represent ± SEM. * $p < 0.05$, ** $p < 0.01$, *** $p < 0.001$. 4-hydroxytamoxifen, 4-OHT; sacrifice, Sac; Contextual Fear Conditioning, CFC; control, Ctrl; Alzheimer's disease, AD; percent, %; enhanced yellow fluorescent protein, EYFP; dentate gyrus, DG.

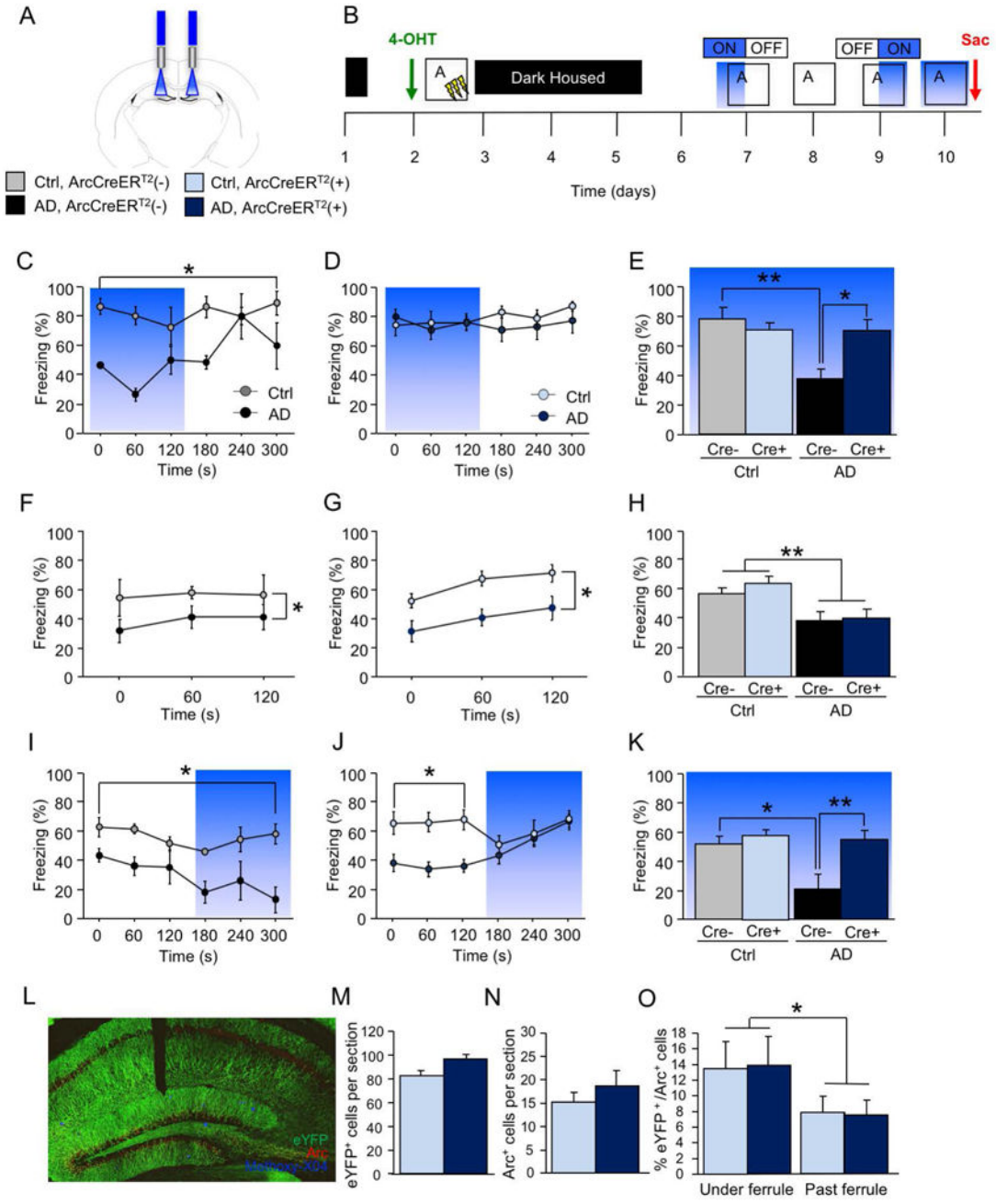

Figure 6. Optogenetic stimulation of a DG memory trace improves memory retrieval in AD mice

(A) Schematic of the bilateral ferrule placement.

(B) Behavioral schematic. Context A memory traces are labeled after a 4-OHT injection.

(C) Freezing in Context A is not impacted by optogenetic stimulation of the aversive A memory trace in ArcCreER^{T2}(-) × ChR2-EYFPxAPP/PS1 (Cre- AD) mice.

(D) Freezing in Context A is significantly increased by optogenetic stimulation of the aversive A memory trace in ArcCreER^{T2}(+) × ChR2-EYFP × APP/PS1 (Cre+ AD) mice.

(E) Cre- AD mice freeze significantly less than Cre- Ctrl mice. Optogenetic stimulation of the aversive A memory trace increases freezing in Cre+ AD mice when compared with Cre- AD mice.
(F-H) Cre- and Cre+ AD mice freeze significantly less than do Cre- and Cre+ Ctrl mice during context A test without optogenetic stimulation.
(I) Optogenetic stimulation of the aversive A memory trace does not impact freezing behavior in Cre- AD mice when compared with Cre- Ctrl mice.
(J) Optogenetic stimulation of the aversive A memory trace increases freezing in Cre+ AD mice to levels similar to those of Cre+ Ctrl mice.
(K) Cre- AD mice freeze significantly less than Cre- Ctrl mice. Optogenetic stimulation of the aversive A memory trace increases freezing in Cre+ AD mice when compared with Cre- AD mice.
(L) Representative image of ferrule placement.
(M-N) There was no effect of Genotype on the number of $EYFP^{+}$ or the number of Arc^{+} cells during optogenetic stimulation.
(O) Stimulation increased co-labeling directly under the ferrule for both Cre+ AD and Ctrl mice. (n = 4-5 male mice per group). Error bars represent ±SEM. * $p < 0.05$, *** $p < 0.0001$. Control, Ctrl; Alzheimer's disease, AD; dentate gyrus, DG; enhanced yellow fluorescent protein, EYFP; percent, %, 4-hydroxytamoxifen, 4-OHT; seconds, s; $ArcCreER^{T2}(-)$, Cre-; $ArcCreER^{T2}(+)$, Cre+.